작은 직류링크 커패시터를 갖는 단상 다기능 온보드 배터리 충전기

누옌황부, 이동춘
영남대학교 전기공학과

Single-Phase Multifunctional Onboard Battery Charger with Small DC-link Capacitors

Hoang Vu Nguyen and Dong-Choon Lee
Department of Electrical Engineering, Yeungnam University

ABSTRACT

In this paper, a single-phase multifunctional onboard battery charger with small DC-link capacitors is proposed, where the low-voltage battery charger is utilized as an active power filter to mitigate the inherent second-order ripple power when the high-voltage (HV) battery is charged from the grid. In this scheme, the large DC-link electrolytic capacitors of the HV battery charger can be eliminated without additional switches, leading to the reduction of cost and volume of the onboard battery charger. The validity of the proposed topology has been verified by the simulation results.

1. Introduction

In plug-in electric vehicles (EVs), their battery is charged from the grid via onboard battery charger by connecting to the AC grid. In general, there are two kinds of batteries in the EVs. One is the HV battery for traction motors and the other is the low-voltage (LV) battery for auxiliary power supplies feeding the loads such as lighting and signaling circuits, entertainments, automatic seats, and other electronic devices. Instead of alternators in the conventional vehicle with an internal combustion engine, this battery is charged from the HV battery through the auxiliary charger system. The onboard battery chargers usually require a long life cycle, small volume and light weight [1].

In the meanwhile, there is a critical problem of second-order ripple power in single-phase onboard battery chargers. Usually, bulky electrolytic capacitors are used to absorb this pulsating power so that the DC voltage is kept relatively constant. This, however, results in a large converter size, consequently, low power density. In recent, a large number of active methods have been suggested to reduce the DC-link capacitance requirement, hence the film capacitors can be used instead of electrolytic capacitors [2], [3]. Unfortunately, the auxiliary circuit with active components is required, which increases the power loss, cost, and complexity of the system.

This paper proposes a multifunction onboard battery charger for EVs with small DC-link capacitors. When the charger is operated in G2V or V2G modes, the LV battery charging circuit functions as an active filter to eliminate the low-frequency ripple power at the DC link. Therefore, small film capacitors on the primary side of LV charger can be employed instead of large electrolytic capacitors at the DC link. With the proposed LV battery charger with the active power decoupling function, the size and cost of the onboard battery charger can be reduced significantly without additional switching devices. The simulation results verify the validity of the proposed system.

2. Circuit Configuration and Control Scheme

2.1 *Proposed multifunctional onboard battery charger*

The circuit configuration of the proposed multifunctional battery charger is shown in Fig. 1. When the SW_1 is ON, the system is operated in either G2V or V2G modes, where the HV battery is charged from the gird or discharged to release power back to the grid. In the meanwhile, the SW_2 is switched to point "a", and the hybrid DC-DC converter (HDC) works as an active power decoupling (APD) circuit to absorb the inherent power ripple in the single-phase system. When the SW_1 is OFF, the SW_2 is connected to point "b". In this case, the HDC works as the half-bridge isolated DC-DC converter to charge the LV battery from the HV battery.

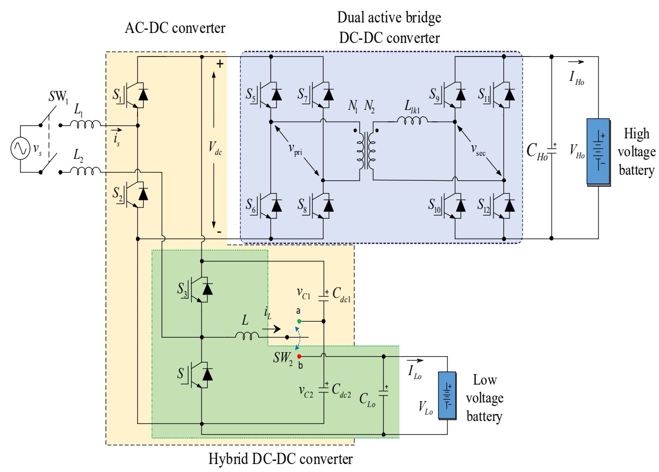

Figure 1. Circuit configuration of the proposed multifunctional charger.

2.2 *Proposed hybrid LV battery charger circuit with active power decoupling function*

In order to achieve the APD function, the LV charger is connected at the DC link of the HV charger, rather than being connected directly to the HV battery. When the HDC is operated as an LV battery charger, it is operated as a half-bridge isolated DC-DC converter to charge the LV battery. When the HDC acts as an APD circuit, an auxiliary inductor, L_r , is added. Then, the symmetrical half-bridge circuit composed of two identical capacitors on the primary side of LV charger, $C_{dc1} = C_{dc2} = C_f$, and a small inductor, L_r, is operated as active power filter. The relay, SW_2, is used for switching between APD function and LV battery charging. As a result, the APD capability is obtained. It should be noted that the switching devices of AC-DC converter in this circuit is the same as that of conventional H-bridge AC-DC converter. Therefore, one converter leg is saved compared with the charger shown in [4].

3. Control Method for Proposed Battery Chargers

3.1 *G2V and V2G modes*

To analyze the power flow in the circuit, the grid voltage and current are expressed as

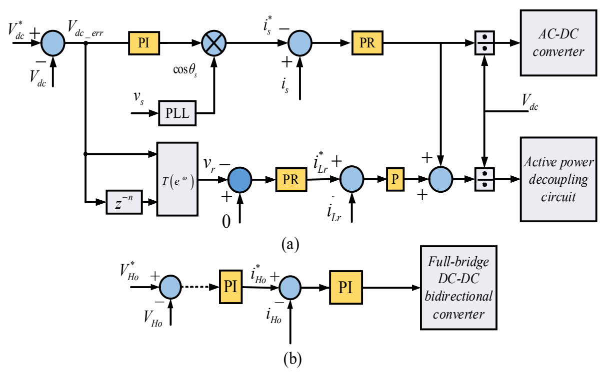

Figure 2. Control block diagram of the proposed battery charger in G2V and V2G modes. (a) For AC-DC converter. (b) For DAB converter.

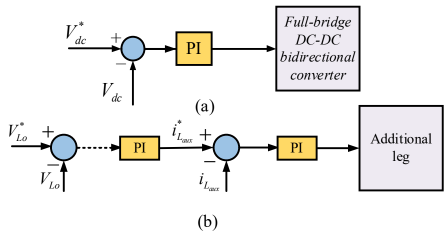

Figure 3. Control block diagram of the proposed battery charger in H2L mode. (a) For bidirectional DC-DC converter. (b) For hybrid DC-DC converter.

TABLE I. PARAMETERS OF EV CHARGING SYSTEM

Parameters	**Value**
HV charger	3.3 kW
LV charger	1 kW
DC output voltage	220 V
Input voltage	220 V (RMS) 60 Hz
C_f	300 uF
L_r	1.5 mH
Transformer turn ratio	1.75:1
HV battery voltage	250 V
LV battery voltage	24 V
C_{aux}	200 uF
C_{Ho}	200 uF
Switching frequency	10 kHz
L_{s1}, L_{s2}	1.5 mH
L_k	100 uH

$$v_s = \sqrt{2}V_s \sin(\omega t) \tag{1}$$

$$i_s = \sqrt{2}I_s \sin(\omega t) \tag{2}$$

where V_s and I_s are the rms values of the input voltage and current, respectively, and ω is the line angular frequency.

For a simple analysis, the filter inductance is not considered and the circuit is assumed to be lossless. In this case, the instantaneous input power is expressed as

$$p_s = V_s \sin(\omega t) \times I_s \sin(\omega t) = \frac{V_s I_s}{2} - \frac{V_s I}{2}\cos(2\omega t) \tag{3}$$

In (3), there is an inherent oscillating power term. In order to decouple the ripple power component, the upper and lower capacitor voltages need to be modified, respectively, as

$$v_{C1}^* = \frac{V_{dc}}{2} - \sqrt{2}V_c \cos(\omega t + \varphi) \tag{4}$$

$$v_{c2}^* = \frac{V_{dc}}{2} + \sqrt{2}V_c \cos(\omega t + \varphi) \tag{5}$$

where the amplitude, V_c and the phase angle, φ, of the

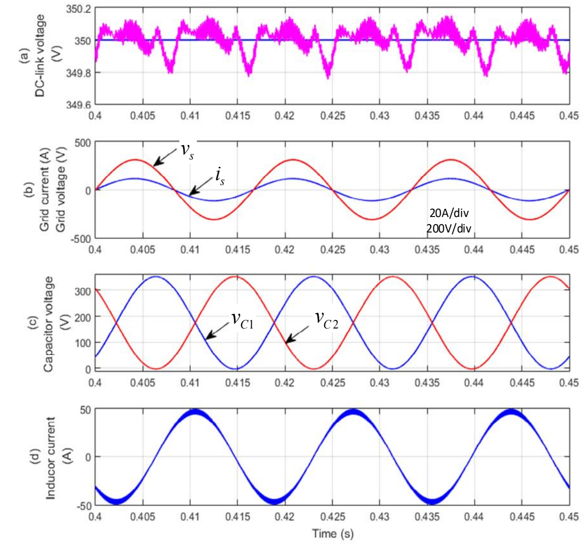

Figure 4. Control of battery charger in G2V mode. (a) DC-link voltage. (b) Grid current and voltage. (c) Capacitor voltages. (d) Inductor current.

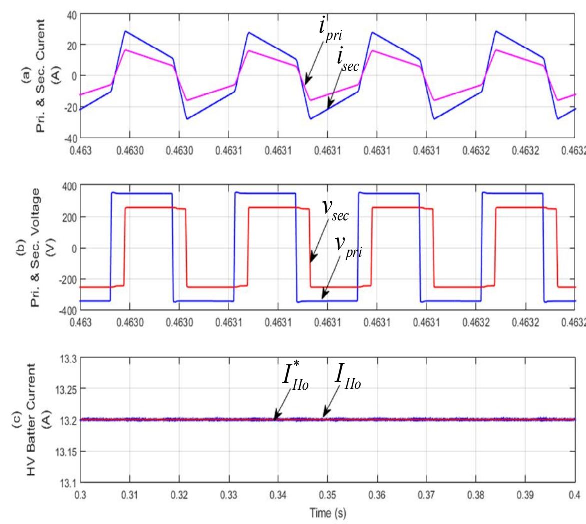

Figure 5. Control performance of DC-DC converter at constant-current charging profile. (a) Primary and secondary currents of DAB. (b) Primary and secondary voltages of DAB. (c) HV battery current.

compensated components are derived, respectively, as [4]

$$V_c = \sqrt{\frac{V_s I_s}{2\omega C_f}} \tag{6}$$

$$\varphi = \frac{1}{2}\arctan\left(-\frac{V_s}{\omega V_s I_s}\right). \tag{7}$$

Then, the ripple power can be absorbed by the two decoupling capacitors, which does not appear in the DC link. However, it is very difficult to achieve the perfect power decoupling if there are parameter uncertainties and disturbances in the system. Therefore, the closed-loop control is applied to solve this issue [5].

Fig. 2 show the control block diagram of the AC-DC converter and APD circuit in V2G mode, where the PR controller is used to control the source current. For the DC-link voltage control, the PI regulator is used. The aim of the APD circuit is to force the ripple component in the DC link to be zero. Therefore, this ripple is mitigated by the PR controller. Then, the output of this PR controller makes the reference for the inner current control loop, where only a P gain is used. Fig. 2(b) shows the control block diagram for charging the HV battery, where the constant current -

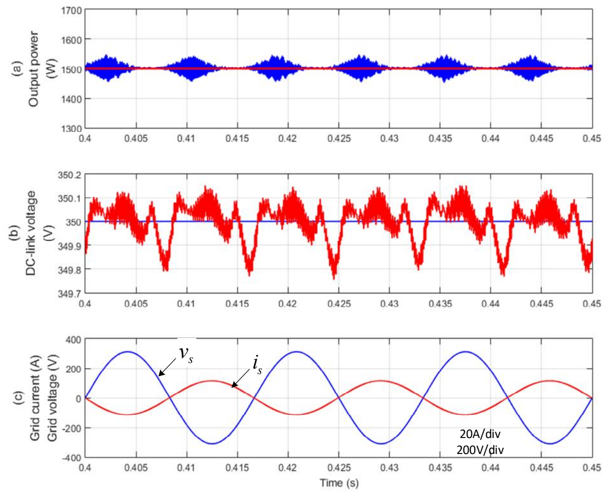

Figure 6. Control of battery charger in V2G mode. (a) HV battery current (b) DC-link voltage. (c) Grid current and voltage.

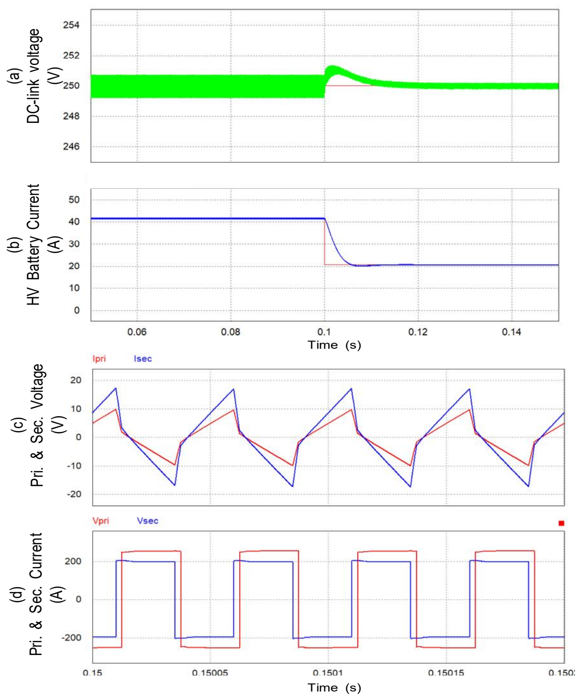

Figure 7. Control of battery charger in H2L mode. (a) DC-link voltage. (b) LV battery voltage. (c) Primary and secondary currents of DAB. (b) Primary and secondary voltages of DAB.

constant voltage (CC-CV) is applied with the PI controllers.

In the V2G mode, the DAB is used to manage the HV battery power. The DC-link voltage and grid current are controlled by the AC-DC converter, in which the closed-loop control is also adopted, where the controllers are the same as those of Fig. 2(a) except that the signs of DC-link voltage and grid current are reversed.

3.2 *LV Battery charging function – H2L mode*

When the SW_1 is OFF, the vehicle is disconnected to the grid. This time, the SW_2 is connected to terminal "b", and the hybrid converter operates as a half-bridge isolated DC-DC converter to charge the LV battery. Fig. 3 shows the control block diagram for charging the LV battery from the HV battery. In this mode, the DC-link voltage is controlled by the bidirectional DC-DC converter, where the PI controller is adopted, as shown in Fig. 3(a). For control of the LV battery charger, the PI controller is used, where the phase-shift modulation is applied to generate the gating signal for the half-bridge isolated DC-DC converter, as shown in Fig. 3(b).

3. Simulation Results

To verify the effectiveness of the proposed circuit, the PSIM simulation has been carried out for a 3.3 kW system. The system parameters are listed in Table I.

Fig. 4 shows the simulation results of the proposed battery charger in G2V mode, in which the DFC works as an APC circuit. It can be seen from Fig. 4(a) that the DC-link voltage ripple is about 0.2% compared with the average voltage value of 350 V. The input current and voltage are shown in Fig. 4(b), where the input current is controlled to be sinusoidal at unity power factor. Fig. 4 (c) shows the upper and lower capacitor voltages which are sinusoidal. They match well with the theoretical analysis. The inductor current is shown in Fig. 4(d) and its peak value is about 45A.

Fig. 5 shows the control performance of the DAB converter at a constant-current charging condition. The currents and voltages of the DAB converter are shown in Fig. 5(a) and (b), respectively. In this case, the power flows from primary side to secondary side of the DAB converter. Fig. 5(c) shows the HV battery charging current, which is well regulated at 13.2A.

Then, the operation of the proposed charger in V2G mode is shown in Fig. 6. The HV battery power is controlled by the DAB converter, as shown in Fig. 6(a). The DC-link voltage is controlled well by the ripple of about 0.2% compared with the average voltage value, as shown in Fig. 6(b). Fig. 6(c) shows the typical waveforms during V2G mode, where the grid current is controlled to be sinusoidal.

Finally, Fig. 7 shows the typical operating waveforms during the H2L mode. The DC-link voltage is well controlled at 250 V as shown in Fig. 7(a). The LV battery current and is shown in Fig. 7(b), which are well controlled at their references. The currents and voltages of the DAB converter are shown in Fig. 7(d) and (e), respectively.

5. Conclusions

In this paper, a multifunction onboard battery charger for EVs with small DC-link capacitors has been proposed, which can operate in three different modes. The proposed charger system utilizes the common components for the LV battery charger and the APD circuit. Therefore, the charger can operate with APC function without adding additional switches, heat sink, and corresponding gated circuit. As a result, the DC-link capacitor can be reduced to one tenth that of the conventional passive approach, so that the small film capacitor can be used at the DC-link. The effectiveness of the proposed system has been verified by the simulation results.

Acknowledgment

This research was supported by the National Research Foundation of Korea grant (NRF-2017R1A2A2A05069629) funded by the Korea government.

References

[1] S. Haghbin, S. Lundmark, M. Alakula, and O. Carlson, "An isolated high-power integrated charger in electrified-vehicle applications," *IEEE Trans. Veh. Technol.*, vol. 60, no. 9, pp. 4115–4126, Nov. 2011.

[2] H. Hu, S. Harb, N. Kutkut, I. Batarseh, and Z. J. Shen, "A review of power decoupling techniques for microinverters with three different decoupling capacitor locations in PV systems," *IEEE Trans. Power Electron.*, vol. 28, no. 6, pp. 2711–2726, Jun. 2013.

[3] Y. Sun, Y. Liu, M. Su, W. Xiong, and J. Yang, "Review of active power decoupling topologies in single-phase systems," *IEEE Trans. Power Electron.*, vol. 31, no. 7, pp. 4778–4794, Jul. 2016.

[4] H. V. Nguyen and D.-C. Lee, "Single-phase multifunctional onboard battery chargers with active power decoupling capability," in *2018 IEEE Applied Power Electronics Conference and Exposition (APEC)*, 2018, pp. 3434–3439.

[5] Y. Tang and F. Blaabjerg, "A component-minimized single-phase active power decoupling circuit with reduced current stress to semiconductor switches," *IEEE Trans. Power Electron.*, vol. 30, no. 6, pp. 2905–2910, 2015.